

1 **Title:** Detecting Glaucoma Worsening Using Optical Coherence Tomography Derived

2 Visual Field Estimates

3 **Authors:** Alex T. Pham¹, Chris Bradley¹, Kaihua Hou², Patrick Herbert², Mathias

4 Unberath, Pradeep Y. Ramulu¹, Jithin Yohannan^{1,2}

5 ¹Wilmer Eye Institute, Johns Hopkins University School of Medicine, Baltimore, MD,

6 USA.

7 ²Malone Center for Engineering in Healthcare, Johns Hopkins University, Baltimore,

8 Maryland

9 **Corresponding author:** Jithin Yohannan, MD MPH

10 Wilmer Eye Institute, Johns Hopkins Hospital

11 600 N. Wolfe St., Baltimore, MD 21287, USA

12 jithin@jhmi.edu

13 **Meeting Presentation:** Association for Research in Vision and Ophthalmology (ARVO)

14 2023

15 **Financial Support:** Supported by grants from the National Institute of Health

16 1K23EY032204-02, Research to Prevent Blindness Unrestricted Grant, BrightFocus

17 Foundation G2023010S, and ARVO Epstein Award

18 **Conflict of Interest:** None relevant

- 19 **Running head:** Detecting glaucoma progression with OCT-derived VF estimates
- 20 **Reprint Address:** Wilmer Eye Institute, Johns Hopkins Hospital, 600 N. Wolfe St.,
- 21 Baltimore, MD 21287, USA.

22 **Abstract**

23 **Objective:** Multiple studies have attempted to generate visual field (VF) mean deviation
24 (MD) estimates using cross-sectional optical coherence tomography (OCT) data.

25 However, whether such models offer any value in detecting longitudinal VF progression
26 is unclear. We address this by developing a machine learning (ML) model to convert
27 OCT data to MD and assessing its ability to detect longitudinal worsening.

28 **Design:** Retrospective, longitudinal study

29 **Participants:** A model dataset of 70,575 paired OCT/VFs to train an ML model
30 converting OCT to VF-MD. A separate progression dataset of 4,044 eyes with ≥ 5
31 paired OCT/VFs to assess the ability of OCT-derived MD to detect worsening.

32 Progression dataset eyes had two additional unpaired VFs (≥ 7 total) to establish a
33 “ground truth” rate of progression defined by MD slope.

34 **Methods:** We trained an ML model using paired VF/OCT data to estimate MD
35 measurements for each OCT scan (OCT-MD). We used this ML model to generate
36 longitudinal OCT-MD estimates for progression dataset eyes. We calculated MD slopes
37 after substituting/supplementing VF-MD with OCT-MD and measured the ability to
38 detect progression. We labeled true progressors using a ground truth MD slope <0.5
39 dB/year calculated from ≥ 7 VF-MD measurements. We compared the area under the
40 curve (AUC) of MD slopes calculated using both VF-MD (with <7 measurements) and
41 OCT-MD. Because we found OCT-MD substitution had a statistically inferior AUC to
42 VF-MD, we simulated the effect of reducing OCT-MD mean absolute error (MAE) on the
43 ability to detect worsening.

44 **Main Outcome Measures:** AUC

45 **Results:** OCT-MD estimates had an MAE of 1.62 dB. AUC of MD slopes with partial
46 OCT-MD substitution was significantly worse than the VF-MD slope. Supplementing VF-
47 MD with OCT-MD also did not improve AUC, regardless of MAE. OCT-MD estimates
48 needed an MAE ≤ 1.00 dB before AUC was statistically similar to VF-MD alone.

49 **Conclusion:** ML models converting OCT data to VF-MD with error levels lower than
50 published in prior work (MAE: 1.62 dB) were inferior to VF-MD data for detecting trend-
51 based VF progression. Models converting OCT data to VF-MD must achieve better
52 prediction errors (MAE ≤ 1 dB) to be clinically valuable at detecting VF worsening.

53 **Keywords:** mean deviation, estimate, optical coherence tomography, visual field

54 **Abbreviations and Acronyms:** VF, visual field; MD, mean deviation; dB, decibels;
55 OCT, optical coherence tomography; RNFL, retinal nerve fiber layer; ML, machine
56 learning; MAE, mean absolute error; SVM, support vector machine; AUC, area under
57 the curve

58

59 **Introduction**

60 Early detection of glaucoma progression is critical to manage the disease effectively.
61 Identifying those at the highest risk of progression allows clinicians to adjust therapy
62 before additional irreversible vision loss occurs. Glaucoma monitoring is usually done by
63 tracking structural changes with optical coherence tomography (OCT) imaging and
64 functional changes with visual field (VF) testing. Since OCT imaging and VF testing
65 have their respective advantages and disadvantages that make either alone less than
66 ideal for detecting progression, they are often used in combination. In general, there are
67 differences in the ability of VF and OCT to detect glaucoma worsening at various stages
68 of the disease. OCT is more sensitive to detecting disease progression in earlier stages
69 of glaucoma. At the same time, VF is more informative at later stages when structural
70 features reach the measurement floor of the OCT instrument.¹⁻⁷

71 There are multiple approaches to addressing the difference between OCT and VF to
72 monitor progression. While clinicians are skilled at monitoring progression using their
73 own experience and judgment, it has been suggested that OCT could help guide VF
74 testing by focusing on measuring functional changes in regions with significant
75 structural changes as the structure-function relationship demonstrates better agreement
76 with regional or sectoral measurements.⁸ Another approach involves using structural
77 information from OCT, such as the retinal nerve fiber layer (RNFL), to predict functional
78 measures, such as mean deviation (MD).⁹⁻¹⁶ The appeal of this pursuit is that it relates
79 different measurement scales (microns per year versus dB per year), and it provides a
80 “functional” measure while retaining the inherent clinical advantages of OCT, such as

81 better repeatability, reproducibility, objectivity, and sensitivity to early glaucomatous
82 damage.^{3-5,17-20}

83 Due to the growing availability of large datasets from electronic health records, most
84 recent efforts to predict MD from OCT (OCT-MD) have focused on applying deep
85 learning models to optic nerve head OCT scans, macular OCT scans, or both.^{9-14,16}
86 However, the OCT-MD estimations from these models have limited accuracy, with
87 mean absolute errors (MAE) ranging from 2-5 dB^{9-14,16}The test-retest variability of MD
88 measurements from VF (VF-MD) is less than 1.5 dB.^{21,22} The best-performing structure-
89 function models in the work mentioned above report MAEs of approximately 2 dB. It is
90 likely that OCT-MD alone cannot predict progression with the same accuracy as VF, but
91 this has yet to be assessed. Additionally, OCT-MD estimates could still have clinical
92 utility if assessed in combination with VF measurements. This is relevant because
93 patients often alternate between OCT and VF and frequently have both available for the
94 clinician to assess progression. Assuming at least five VFs are needed to calculate a
95 reliable MD rate of change for monitoring trend-based progression, the ability to
96 substitute VF-MD with OCT-MD would reduce the testing burden on patients and allow
97 clinicians to determine the rate of change more quickly, leading to earlier detection of
98 progression.^{23,24} This is especially important since treatment decisions must often be
99 made only after a few visits.

100 Hence, the aims of our study are two-fold. First, our study aimed to evaluate whether
101 OCT-MD has any clinical value as a substitute for VF-MD (either through complete or
102 partial substitution) to detect trend-based glaucoma progression with non-inferior
103 accuracy to VF-MD alone. Second, if we find that OCT-MD estimates, with an MAE

104 similar to or better than prior published work, are not accurate enough to be clinically
105 viable, we aimed to determine the MAE needed for OCT-MD to be useful in trend-based
106 analysis. Currently, there is no established evidence-based MAE threshold that
107 investigators developing these models should aim to stay below. Thus, knowing the
108 maximum acceptable error level would clarify the ideal goal for modeling the structure-
109 function relationship to detect functional change over time.

110 **Methods**

111 Our study adhered to the Declaration of Helsinki and was approved by the Johns
112 Hopkins University School of Medicine Institutional Review Board.

113 *Study Population and Data Collection*

114 Adult patients with a glaucoma or glaucoma-related diagnosis followed at the Wilmer
115 Eye Institute Glaucoma Center of Excellence from April 2013 to July 2022 were
116 considered eligible for our study. From these eligible eyes, we created a dataset to train
117 and test a machine learning model to estimate OCT-MD, referred to as the “model
118 dataset”, and a separate dataset to evaluate the ability to predict VF worsening from
119 trend-based analysis of the OCT-MD generated by the model, referred to as the
120 “progression dataset”. The same eye or patient was never present in both datasets. For
121 the progression dataset, the inclusion criteria were eyes with 5 or more reliable VFs
122 (reliability criteria defined below), each paired with a reliable optic nerve head OCT scan
123 (reliability criteria defined below) taken within a 1-year time window. Each pairing was
124 unique in that there were no overlapping VFs or OCTs among the pairings. These eyes
125 also had to have 2 additional unpaired VF tests. The rationale for these inclusion criteria

126 was based on the notion that at least 5 VF tests are needed to calculate a reliable MD
127 slope^{23,24}, and the additional 2 unpaired VF tests were used to establish a ground truth
128 for the rate of progression. Hence, each eye in the progression dataset had 7 or more
129 VFs. For the model dataset, the inclusion criteria were peripapillary OCT scans and VF
130 tests obtained from eyes with less than 7 VFs over time, so there are no overlapping
131 eyes between the progression and model dataset. OCT scans and VF tests also had to
132 be paired within one year of each other. Only reliable OCT scans and reliable VF tests
133 were considered during the construction of the model dataset as well.

134 For OCT scans to be considered reliable, they had to have a signal strength > 6, and
135 average, superior quadrant, and inferior quadrant RNFL thickness measurements
136 between 57 to 135, 175, and 190 μm , respectively. An RNFL floor of 57 μm was used
137 because values below this threshold are likely due to artifact or segmentation error.^{25,26}
138 Moreover, it is unlikely any further longitudinal changes can be observed in eyes that
139 have reached the OCT floor.²⁷ An RNFL ceiling of 135, 175, and 190 μm was used for
140 the average, superior, and inferior thickness, respectively, because these thresholds are
141 approximately three standard deviations above the average RNFL thickness measured
142 in normal healthy eyes.²⁸ All OCT studies were obtained using CIRRUS HD-OCT
143 (Zeiss, Dublin, CA).

144 To be considered reliable, VFs had to have false positive rates < 15% for all stages of
145 disease, false negative rates < 25% for suspect or mild glaucoma, and false negative
146 rates < 50% for advanced glaucoma.²⁹ All VF tests were performed using the Humphrey
147 Visual Field Analyzer II or III with the SITA Standard, Fast, or Faster testing algorithm
148 and the 24-2 pattern. Only VF tests with MD measurements better than -10.4 dB were

149 included in the study because MDs worse than -10.4 dB likely indicate that the eye has
150 reached the RNFL floor.²⁷ Since our study aims to assess the feasibility of detecting
151 progression with OCT-derived MD, the rationale for this restriction is to provide the most
152 favorable conditions that would produce the most accurate conversion estimates. If the
153 progression cannot be accurately detected using estimates limited to the dynamic range
154 of OCT, it is unlikely to have the potential for clinical utility in real-world circumstances.
155 Variables collected for our study included age, gender, race, and glaucoma severity.
156 Glaucoma severity was determined using the MD measurement from the first VF
157 available for each eye. Eyes with a baseline MD better than -6 dB and between -6 and
158 -10.4 dB were considered suspect/mild and moderate glaucoma, respectively. Eyes
159 with an MD better than -6 dB were considered glaucoma suspect, as opposed to mild
160 glaucoma, if their glaucoma hemifield test was “within normal limits”.

161 *Estimating VF Mean Deviation from Optic Nerve OCT Characteristics in the Model*

162 *Dataset*

163 Using the model dataset, we investigated multiple machine-learning models to estimate
164 MD based on various features measured by OCT scans of the optic disc. Input features
165 for each model were the average RNFL thickness, four quadrant RNFL thicknesses
166 (superior, inferior, nasal, temporal), 12 clock hour RNFL thicknesses, 6 Garway-Heath
167 Zone RNFL thicknesses, cup volume, disc area, rim area, average cup-to-disc ratio,
168 vertical cup-to-disc ratio, signal strength, and baseline age. Classical machine learning
169 algorithms that were tested included random forest, support vector machine (SVM)
170 regression, lasso regression, and K-nearest neighbors. We also tested deep learning
171 models such as convolutional neural networks, multi-layer perceptron, and a model

172 combining both previous neural networks. A training and testing set were created using
173 an 80:20 percent split of the model dataset described above. Hyperparameters were
174 optimized by comparing the performance of various combinations of parameters after
175 cross-validation on the training set. We used 5-fold cross-validation, which involves
176 randomly splitting the training set into five non-overlapping folds of equal size. The
177 model was then trained on a combination of four folds while the remaining fold, a
178 holdout set, was used for validation to evaluate performance. An evaluation score was
179 obtained from this holdout set, and this process was repeated five times so that each
180 fold had an opportunity to be used once for validation. The model's performance for a
181 particular combination of hyperparameters was then summarized by taking the average
182 of the evaluation scores from the five iterations. The combination of parameters that
183 produced the strongest average evaluation score after cross-validation was used as the
184 optimal parameters for the model. Afterward, the performance of each optimized model
185 was evaluated by generating an OCT-MD from each paired OCT scan in the test set
186 and calculating the mean absolute error (MAE) between the OCT-MD estimate and the
187 real MD measurement, VF-MD. The optimized model with the lowest MAE obtained
188 from the test set was used to predict disease progression described in the following
189 section.

190 *Detecting Glaucoma Progression in the Progression Dataset*

191 An overview of our study method can be seen in Figure 1. After constructing a model to
192 generate OCT-MD, an MD estimate was obtained from each paired OCT scan for each
193 eye in the progression dataset. We evaluated the utility of using these OCT-MD
194 estimates with VF-MD to detect trend-based glaucoma progression. Our primary

195 approach involved selecting a random subset of the longitudinal VF-MD measurements,
196 replacing them with their paired OCT-MD estimates, and calculating the MD slope using
197 ordinary least squares regression. We refer to this approach of combining OCT-MD and
198 VF-MD as ‘substitution’. The MD slope calculation from substitution is referred to as the
199 ‘VF-MD/OCT-MD slope’. Varying amounts of VF-MD substitutions were tested: 20%,
200 40%, 60%, 80%, and 100% substitution. For example, if an eye had ten VF studies with
201 ten paired OCT scans, 80% substitution means that randomly chosen eight VF-MDs
202 were replaced with their paired OCT-MDs.

203 We were also interested in investigating whether OCT-MD could be used to improve the
204 predictive ability of VF-MD when it is included as supplemental information in trend-
205 based analysis. In other words, our secondary approach involved combining all OCT-
206 MD estimates with all paired VF-MD measurements by using OCT-MD as additional
207 data points in the MD slope calculation with ordinary least squares regression. We refer
208 to this approach of combining OCT-MD and VF-MD as ‘addition’. The MD slope
209 calculation from addition is referred to as the ‘VF-MD + OCT-MD slope’.

210 To evaluate the accuracy of the VF-MD/OCT-MD slopes and VF-MD + OCT-MD slopes,
211 we established a “ground truth” MD slope for analysis purposes. The ground truth MD
212 slope was calculated using all available VF studies (at least 7 or more), which equate to
213 two additional data points beyond the time window of the paired VF tests and OCT
214 scans (at least 5 or more) for each eye in the progression dataset. Receiver operating
215 characteristic curves were generated for VF-MD/OCT-MD slopes and VF-MD + OCT-
216 MD slopes using the ground truth MD slope. Eyes with a statistically significant ground
217 truth MD slope ($\alpha = 0.05$) worse than -0.50 dB/year were labeled true progressors.^{30–33}

218 We also repeated the analysis to determine whether OCT-MD could predict slower and
219 faster rates of VF worsening by using MD slope cut-offs of -0.25 , -0.75 , and -1.00
220 dB/year. The area under the receiver operating characteristic curve (AUC) was used to
221 evaluate the performance of the VF-MD/OCT-MD and VF-MD + OCT-MD slopes.

222 To compare the VF-MD/OCT-MD slopes derived from substitution to VF-MD, we
223 calculated an MD slope when no VF-MDs were substituted, which we will refer to as the
224 baseline VF-MD slope. The VF-MD/OCT-MD slopes for 20%, 40%, and 60%
225 substitution were also compared to baseline VF-MD slopes calculated using 20%, 40%,
226 and 60% fewer VFs to determine whether partial substitution with OCT-MD does better
227 than simply using fewer VFs to calculate MD slope. Statistical comparisons between the
228 AUCs of the MD slopes were made using Delong's test.

229 *Accuracy Needed to Predict Progression with OCT- MD*

230 After evaluating the performance of VF-MD/OCT-MD and VF-MD + OCT-MD slopes in
231 predicting progression, we investigated the impact of OCT-MD MAE on the AUCs. It is
232 currently unknown what MAE is needed for OCT-MD estimates to be viable when used
233 alone or combined with VF-MD in trend-based analysis to detect progression. To
234 simulate OCT-MD model estimates with a lower MAE, we took the original MAE of our
235 model and calculated the error percent reduction needed to lower it to 1.50, 1.25, 1.00,
236 0.75, and 0.50 dB. Then, we calculated the residual error between the paired OCT-MD
237 and VF-MD for the eyes in our progression dataset. The OCT-MD estimates were
238 brought closer to the paired VF-MD measurements by artificially reducing the residual
239 error between them by the percentages calculated above. As an example, if the original
240 MAE of our model was 2.00 dB, the percent reduction needed to achieve an MAE of

241 1.50 dB would be 25%. If the original OCT-MD estimate was -2.00 dB and the paired
242 VF-MD was -1.00 dB, the residual error would be 1.00 dB. A 25% reduction of the
243 residual would lead to a simulated OCT-MD estimate of -1.75 dB. MD slopes were
244 recalculated using these simulated OCT-MD estimates, and the AUC analysis was
245 repeated.

246 *Sensitivity Analyses*

247 We conducted two sensitivity analyses. First, since our current inclusion criteria allow
248 OCT scans and VFs to be paired up to one year apart, this may introduce temporal bias
249 in the model. The OCT-MD produced by the model could be estimating a VF-MD one
250 year ahead or behind the OCT scan date, which may affect our analysis of longitudinal
251 changes to predict progression. To address this concern, we conducted a sensitivity
252 analysis by training our machine learning model on only OCT scans and VF tests that
253 were paired on the same day. In addition, when using the OCT-MD estimates to detect
254 glaucoma progression, we only analyzed eyes with 5 or more OCT scans and VF tests
255 also paired on the same day. Second, we investigated including confidence intervals
256 when labeling true progressors since OCT-MD may not be able to detect progression in
257 those with noisier VF tests. The confidence interval for a statistically significant MD slope
258 had to be within a 0.50 dB range (± 0.25 dB of the slope) to be considered as a true
259 progressor.

260 **Results**

261 Baseline demographics, VF, and OCT characteristics for the model and progression
262 datasets are shown in Table 1. The model dataset consisted of 70,575 paired optic disc

263 OCT scans and VF studies obtained from 44,659 eyes, each with less than 7 reliable
264 VFs. The progression dataset consisted of 4,044 eyes with at least 7 reliable VFs, with
265 all but the last 2 VFs paired with OCT. The mean (SD) duration of time between OCT
266 scans and VF studies for each pair was 102 (117) days. The mean age was slightly
267 older in the progression dataset than in the model dataset (64 vs. 62 years, $p < 0.001$).
268 Race, gender, and baseline glaucoma severity were similar for both datasets. Mean MD
269 was slightly worse in the model dataset than in the progression dataset (-1.86 vs. -1.59
270 dB, $p < 0.001$). Pattern standard deviation was slightly better in the model dataset than
271 in the progression dataset (2.46 vs. 2.56 , $p = 0.001$). RNFL was slightly thinner (83 vs.
272 86 μm , $p < 0.001$) and CDR slightly larger (0.62 vs. 0.60 , $p < 0.001$) in the progression
273 dataset than the model dataset.

274 Among the different machine learning models evaluated, the SVM model had the lowest
275 MAE and was used for the remainder of the study. Table 2 shows the MAE of the SVM
276 model and the percentage of OCT-MD estimates within 0.25 dB, 0.50 dB, 1.00 dB, 2.00
277 dB, and 4.00 dB of the true MD value. Overall, the MAE was 1.62 dB, and the
278 percentage of estimates with 0.25 dB, 0.5 dB, 1 dB, 2 dB, and 4 dB of error were 11%,
279 21%, 41%, 71%, and 93%, respectively. The estimations became more inaccurate for
280 later stages of disease. The estimates from eyes with suspect and mild glaucoma had
281 an MAE below 2 dB and the highest proportion of estimates within the various margins
282 of error. Estimates from eyes with moderate disease had the worst MAE of 5.55 dB and
283 the lowest proportions within the various margins of error. This trend is also seen in
284 Figure 2, demonstrating that the MAE of OCT-MD estimates increases the further VF-
285 MD is from -1.0 dB.

286 *Ability of MD slope to detect progression when combining VF-MD with OCT-MD*

287 Figure 3 demonstrates the diagnostic ability of VF-MD/OCT-MD slopes (substitution)
288 calculated from various substitution percentages. For an MD slope cutoff of 0.50
289 dB/year, the AUCs (95% CI) for 20%, 40%, 60%, 80%, and 100% substitution are 0.88
290 (0.86 to 0.90), 0.84 (0.81 to 0.86), 0.77 (0.74 to 0.80), 0.70 (0.67 to 0.74), and 0.60
291 (0.58 to 0.64), respectively. The AUC (95% CI) of the baseline VF-MD slope is 0.91
292 (0.90 to 0.93) and corresponds to 0% substitution. The AUC of the baseline VF-MD
293 slopes calculated using 20%, 40%, and 60% fewer VFs is 0.90 (0.88 to 0.92), 0.86 (0.83
294 to 0.88), and 0.77 (0.73 to 0.80). The AUC of 40% to 100% substitution was significantly
295 worse than the baseline VF-MD slope. Although the AUC of 20% substitution was
296 statistically similar to the baseline VF-MD slope with 0% substitution, it was also similar
297 to the AUC of baseline VF-MD slopes calculated using 20% fewer VFs. The AUC of the
298 OCT-MD slope from 40% and 60% substitution was similar to the baseline VF-MD slope
299 calculated using 40% and 60% fewer VFs, respectively, as well. Figure 3 also shows
300 the AUCs for substitution when using faster and slower MD slope cut-offs. The number
301 of progressing eyes using an MD slope cutoff of -0.25 , -0.50 , -0.75 , and -1.00 dB/year
302 were 380, 149, 47, and 19 eyes, respectively.

303 Table 3 shows the AUCs of the VF-MD + OCT-MD slope (addition) compared to the
304 baseline VF-MD slope for various MD slope cutoff thresholds. For an MD slope cutoff of
305 0.50 dB/year, the AUC when using OCT-MD as additional data points is 0.89 (0.87 to
306 0.91) and was statistically similar to the baseline VF-MD slope. VF-MD + OCT-MD
307 slopes were also statistically similar to the baseline VF-MD slope for slower and faster
308 MD-slope cutoffs.

309 *Accuracy Simulation*

310 The diagnostic ability of VF-MD/OCT-MD slopes with an MAE of 1.50, 1.25, 1.00, 0.75,
311 and 0.50 dB is shown in Figure 4. Figure 4 demonstrates that an MAE of 1.25 dB or
312 better is needed for the AUCs of VF-MD/OCT-MD slopes to be above 0.80 for complete
313 and partial substitution. When the MAE was 1.00 dB or better, the performance became
314 nearly identical to VF-MD alone. For an MAE of 1.25 dB or better, 40% substitution had
315 a higher AUC than simply using 40% fewer VFs. On the other hand, the AUC for 60%
316 substitution only became higher than simply using 60% fewer VFs when the MAE was
317 1.50 dB or better.

318 We performed a similar error simulation to evaluate the diagnostic ability of VF-MD +
319 OCT-MD slopes calculated using OCT-MD estimates with an MAE of 1.50, 1.25, 1.00,
320 0.75, and 0.50 dB. We found that regardless of the accuracy of OCT-MD estimates,
321 using OCT-MD as additional data points for MD slope calculation did not improve the
322 AUC compared to using VF-MD alone.

323 *Sensitivity Analyses*

324 In our first sensitivity analysis, we repeated the main analysis using only VF studies and
325 OCT scans performed on the same day to address possible temporal bias introduced
326 when estimating VFs from OCTs paired up to one year apart. The structure-function
327 model had minimal improvement in performance, with an MAE of 1.59 dB for the OCT-
328 MD estimates compared to an MAE of 1.62 dB for the OCT-MD estimates from the
329 original model. We also achieved similar results to our original analysis when examining
330 the predictive ability of the OCT-MD estimates to predict glaucoma progression.

331 However, it is important to note that the sample size for the progression dataset was
332 substantially smaller with the adjusted inclusion criteria compared to the original
333 inclusion criteria (n = 562 vs. n = 4,044).

334 In our second sensitivity analysis, we repeated the main analysis but required
335 progressing eyes to have an MD slope worse than 0.50 dB/year, p-value < 0.05, and
336 confidence intervals to be within +/- 0.25 dB of the calculated slope. Among the 4,044
337 eyes in the progression dataset, 19 were considered progressing using the above
338 criteria. Similar trends were seen. The AUCs of partially substituted VF-MD/OCT-MD
339 slopes were lower than the baseline VF-MD slope and were worse with increasing
340 substitution percentages. VF-MD/OCT-MD slopes with 20% substitution had a similar
341 AUC to the baseline VF-MD slope, but the same was true for VF-MD slopes using 20%
342 fewer VFs. The AUCs of the VF-MD + OCT-MD slope were similar to the baseline VF-
343 MD slope.

344 **Discussion**

345 In this study, we developed a machine learning model trained on optic nerve head OCT
346 measurements to estimate MD with an error (MAE) of 1.62 dB. The error of the OCT-
347 MD estimates increased with increasing disease severity. Completely substituting VF-
348 MD with OCT-MD resulted in significantly lower AUCs compared to using VF-MD alone.
349 Partially substituting only 20% of VF-MD with OCT-MD had a statistically similar AUC
350 compared to using VF-MD alone. However, partial substitution did not perform better
351 than simply using 20% fewer VFs. Using OCT-MD as additional data points with VF-MD
352 for MD slope calculation did not improve the AUC regardless of the MAE. OCT-MD

353 estimates predicted progression as well as VF-MD alone when the MAE was at or
354 below 1.00 dB.

355 *Model Performance for Estimating Mean Deviation*

356 When predicting VF-MD from OCT data, our structure-function SVM model achieved an
357 overall MAE of 1.62 dB. Prior classical machine-learning and deep-learning models
358 were also trained with structured data, such as thickness measurements, and had mean
359 errors ranging from 3 – 5 dB.^{12,34,35} Our MAE also compares well to more recent studies
360 with sophisticated deep learning models incorporating unstructured data from
361 unsegmented OCT images, which contain much more information than tabular RNFL
362 thickness measurements (MAE ranging from 2.3 – 2.8 dB).^{11,36,37} Our findings are also
363 consistent with those of Wong et al. (2022), who compared different machine learning
364 models trained on global RNFL thickness measurements to estimate global VF-MD and
365 found that gradient-boosted decision trees and SVM performed significantly better than
366 other models, including some deep learning models.³⁵

367 Several reasons may explain the better MAE observed in our study compared to
368 previous work. Our structure-function model was trained on a substantially larger
369 dataset (more than 50,000 OCT-VF pairs). It was trained on additional optic nerve
370 features such as cup volume, disc area, rim area, and cup-to-disc ratio, not just RNFL
371 thickness measurements. Unlike previous studies, we limited OCT-VF pairs used to
372 train the model to only those that fall within the dynamic range of the OCT imaging
373 instrument. The poor accuracy and variability of OCT-MD estimates as visual function
374 worsens is well documented, and the reduced dynamic range of RNFL thicknesses in
375 later stages of glaucoma is a frequently cited reason.^{15,34,38} Moreover, limiting our study

376 population to the dynamic range also limits the generalizability of our model. The model
377 was trained on mostly suspect or mild glaucoma, as eyes with more advanced disease
378 would likely fall outside of the dynamic range. The VF measurements from more
379 advanced diseases are known to be much more variable, which could explain the higher
380 MAEs observed in prior studies.^{9-14,16,39}

381 Since our study aimed to evaluate the feasibility of utilizing OCT-MD in trend-based
382 analysis, we decided to use the conditions that would provide the most accurate
383 estimations. Although this means the generalizability of our findings is likely limited to
384 eyes with earlier stages of glaucoma, it is unlikely that including eyes outside the
385 dynamic range, such as those with moderate or advanced glaucoma, would change the
386 main findings of our study. If it is not possible to use OCT-MD to improve the ability to
387 detect progression in eyes with earlier stages of disease, it is unlikely that OCT-MD
388 would be helpful in eyes with later stages of disease where OCT-MD estimations would
389 be even more inaccurate and variable.³⁹

390 *Detecting Glaucoma Progression with OCT Estimated Mean Deviation*

391 Combining OCT-MD with VF-MD, either through substitution or addition, did not
392 significantly improve the ability to detect progression. Completely or partially substituting
393 VF-MD with OCT-MD led to a worse ability to detect progression than using VF-MD
394 alone. Although only substituting 20% of VF-MD led to statistically similar predictions
395 compared to VF-MD alone (AUC of 0.86 vs 0.87), the same could be achieved by
396 simply using 20% fewer VFs when calculating the rate of MD worsening. When using
397 OCT-MD as additional data points to calculate the rate of MD worsening, the AUC was
398 statistically similar to VF-MD alone, regardless of the MAE. However, when MAE was

399 1.00 dB or better, the OCT-MD estimates could be considered for substitution as the
400 performance was similar to VF-MD alone.

401 If a low enough MAE could be achieved, there are multiple potential advantages to
402 being able to convert an RNFL measurement to MD that we could expect. Since
403 patients often alternate between OCT imaging and VF testing, one may detect
404 glaucoma progression earlier since less time is needed to estimate the rate of MD
405 worsening by using both OCT-MD and VF-MD. Being able to substitute VF-MD with
406 OCT-MD in these situations offers great flexibility in the amount and type of testing
407 needed to produce accurate trend assessments. Due to the variability of VF testing,
408 especially for later stages of disease, at least 10 VFs are required to obtain the most
409 accurate progression rate estimate.⁴⁰ Adding OCT-MD as additional data points with
410 VF-MD in these trend-based analyses may also allow one to obtain more accurate
411 progression rate estimates in less time.

412 Despite the numerous efforts directed at developing structure-function models, there is
413 currently no established evidence-based accuracy threshold that investigators can use
414 to validate the clinical utility of their models. Our work demonstrates that OCT-MD
415 estimates with margins of error greater than 1.00 dB did not provide clinical value in
416 detecting glaucoma progression using trend-based analysis, even when combined with
417 VF-MD measurements through partial substitution or addition. Figure 2 demonstrates
418 that only when OCT-MD is used to predict VF-MD measurements within a 0 to -2 dB
419 range the MAE could be better than 1.00 dB. For most clinical situations, detecting VF
420 worsening within such a narrow range would be challenging. In a best-case scenario,
421 current OCT-MD estimates may help detect worsening in pre-perimetric glaucoma.

422 More work is needed to produce OCT-MD estimates that are accurate enough to
423 estimate progression rates. Several improvements can be made to our model to
424 achieve the required accuracy. We only used mainly RNFL thickness measurements to
425 predict MD, but more accurate estimations may be achieved if we develop a deep
426 learning model that utilizes the RNFL thickness measurements and the corresponding
427 raw, unsegmented OCT image. Lazaridis et al. (2022) previously demonstrated that an
428 ensemble model utilizing the OCT image and the RNFL thickness profile had
429 approximately a 22% lower MAE than a model using only the RNFL thickness profile.³⁷
430 They suggested that OCT images contain additional information, such as vascular
431 features that may be relevant to the structure-function relationship, as retinal ganglion
432 cell loss in glaucomatous eyes with VF damage is associated with decreased regional
433 retinal blood flow.^{41,42} Indeed, some studies have found that combining vasculature
434 measurements from OCT angiography with structural OCT measurements can improve
435 the ability to assess VF defects.^{43,44} Another important structural feature that can
436 improve prediction accuracy is macular information. Yu et al. (2021) found that a deep
437 learning model using both macular and optic nerve head scans had a lower median
438 absolute error for predicting MD than either alone.³⁶ Studies suggest that macular OCT
439 also has a larger dynamic range than optic nerve head OCTs and may be more useful
440 in predicting visual function in the later stages of glaucoma which can potentially help
441 address the poor accuracy observed with structure-function models in later stages of
442 disease and improve generalizability.⁴⁵⁻⁴⁷ Additionally, macular changes can be seen in
443 early glaucoma, and incorporating this information could also further improve the
444 estimations at earlier stages of disease.^{48-50,50-54}

445 Another approach to detecting glaucoma progression using structure-function models
446 that we did not investigate is predicting pointwise VF measurements. In addition to
447 global VF indices, there are efforts to use OCT to estimate individual pointwise VF
448 sensitivities.^{10–12,15,34,37,55} Predicting threshold sensitivities would maintain the spatial
449 relationships between structural features that would not be reflected in an estimated
450 summary metric such as MD. These spatial relationships may help in the early detection
451 of localized disease progression before they can affect the global VF metrics. However,
452 predicting pointwise measurements is a significantly more complex task than predicting
453 global measurements.

454 Since the ultimate goal is to detect disease progression, other approaches that are
455 important to continue investigating are models that predict progression directly rather
456 than computing a VF metric from an OCT metric and then performing a subsequent
457 analysis to predict disease progression. Models utilizing this approach have achieved
458 good performance (AUC > 0.80) in predicting VF worsening from longitudinal OCT
459 information.^{33,56–58} In our previous study, we used a gated-transformer network to
460 predict VF worsening based on MD slope with longitudinal OCT scans.³³ An advantage
461 of this approach is that we could detect spatially dependent structural changes over
462 time with our deep learning model, unlike this study. However, the model is limited by
463 the fact that it requires a minimum of 5 OCT scans as an input (a disadvantage that is
464 not present with the conversion approach). While waiting for enough tests, patients may
465 experience additional vision loss or be lost to follow-up. Consequently, treatment
466 decisions are often needed after only a few visits. These drawbacks also highlight the

467 importance of models identifying future disease worsening with an early or limited
468 diagnostic dataset.⁵⁸

469 There are important limitations to acknowledge in our study. Although our SVM model
470 achieved a low MAE, we only used tabular data from segmented RNFL measurements.
471 As mentioned earlier, it is possible that if we incorporated the unsegmented OCT
472 images, macular OCTs, or OCT angiography into a deep-learning model, we could
473 achieve better MD estimates. We only investigated glaucoma worsening through MD
474 slope but other trend-based analyses such as VFI slope may produce different results.
475 Global VF indices also cannot show spatial relationships, and there is growing evidence
476 that regional or sectoral changes demonstrate better agreement between structure and
477 function.⁸ Predicting pointwise threshold sensitivities rather than global indices may be
478 more useful for evaluating progression in other situations, such as with event-based
479 analysis. When conducting our error simulations, we artificially reduced the residual for
480 each estimate by a certain percentage to mimic a structure-function model with better
481 accuracy, but this assumes that improvements can be made to the model that would
482 improve the accuracy universally among all eyes with differing baseline characteristics
483 and reduce error across all levels of VF damage in the same proportions. Additionally,
484 our structure-function model is trained to predict a single paired VF taken at a single
485 clinic visit and this assumes that the single VF is a true representation of the eye's
486 visual function. However, VF measurements are variable, especially at later stages of
487 disease, and the error observed with the OCT-MD estimates for given measurement will
488 be partly due to this inherent variability. Another approach could involve predicting an
489 average of multiple VF tests as the 'best available estimate' of the true visual function.³⁷

490 However, it would be impractical to obtain multiple VF measurements for each patient
491 on a single visit and do so on a large scale to train a model. The VF studies included
492 are obtained from a mix of testing strategies, and this could potentially confound the MD
493 measurements, but this may only be a limitation for later stages of glaucoma. Prior
494 studies have shown that SITA Faster and SITA Standard perform similarly in mild
495 disease, and performance differences are more pronounced in later stages of
496 disease.⁵⁹⁻⁶³ As the majority of our eyes are suspect or mild glaucoma (93%), we have
497 less concern for measurement bias. Lastly, VF and OCT were paired within one year
498 and this assumes no glaucomatous changes occurred during this timeframe. Although
499 Chauhan et al. (2014) have shown that most eyes have slow rates of VF progression. It
500 is unlikely that significant changes occurred between OCT scans and VF tests.⁶⁴
501 Moreover, our sensitivity analysis utilizing only OCTs and VFs obtained on the same
502 day did not change our results, albeit it could be underpowered.

503 In conclusion, we developed a machine learning model to estimate MD from optic nerve
504 head OCT scans with a low prediction error compared to other structure-function
505 models in the literature. We used the model to estimate VFs from paired OCTs in
506 patients with longitudinal data. We found that even if OCT-MD is combined with VF-MD,
507 either through substitution or addition, it did not improve the ability to detect disease
508 progression compared to VF-MD alone. We conducted an error simulation analysis to
509 determine the accuracy needed for our model to detect glaucoma progression. We
510 found that when the MAE is 1 dB or better, OCT-MD could substitute VF-MD in trend-
511 based analysis. Future work developing structure-function models should aim to

- 512 achieve this lower level of prediction error to ensure the clinical utility of such models to
- 513 detect functional change over time.

514 References

- 515 1. Zhang X, Dastiridou A, Francis BA, et al. Comparison of Glaucoma Progression
516 Detection by Optical Coherence Tomography and Visual Field. *Am J Ophthalmol.*
517 2017;184:63-74. doi:10.1016/j.ajo.2017.09.020
- 518 2. Zhang X, Loewen N, Tan O, et al. Predicting Development of Glaucomatous Visual
519 Field Conversion Using Baseline Fourier-Domain Optical Coherence Tomography.
520 *Am J Ophthalmol.* 2016;163:29-37. doi:10.1016/j.ajo.2015.11.029
- 521 3. Kuang TM, Zhang C, Zangwill LM, Weinreb RN, Medeiros FA. Estimating Lead Time
522 Gained by Optical Coherence Tomography in Detecting Glaucoma before
523 Development of Visual Field Defects. *Ophthalmology.* 2015;122(10):2002-2009.
524 doi:10.1016/j.ophtha.2015.06.015
- 525 4. Wollstein G, Schuman JS, Price LL, et al. Optical coherence tomography
526 longitudinal evaluation of retinal nerve fiber layer thickness in glaucoma. *Arch*
527 *Ophthalmol Chic Ill 1960.* 2005;123(4):464-470. doi:10.1001/archopht.123.4.464
- 528 5. Hood DC, Kardon RH. A framework for comparing structural and functional
529 measures of glaucomatous damage. *Prog Retin Eye Res.* 2007;26(6):688-710.
530 doi:10.1016/j.preteyeres.2007.08.001
- 531 6. Sung MS, Heo H, Park SW. Structure-function Relationship in Advanced Glaucoma
532 After Reaching the RNFL Floor. *J Glaucoma.* 2019;28(11):1006-1011.
533 doi:10.1097/IJG.0000000000001374
- 534 7. Sommer A, Katz J, Quigley HA, et al. Clinically detectable nerve fiber atrophy
535 precedes the onset of glaucomatous field loss. *Arch Ophthalmol Chic Ill 1960.*
536 1991;109(1):77-83. doi:10.1001/archopht.1991.01080010079037
- 537 8. Hood DC. Improving our understanding, and detection, of glaucomatous damage:
538 An approach based upon optical coherence tomography (OCT). *Prog Retin Eye*
539 *Res.* 2017;57:46-75. doi:10.1016/j.preteyeres.2016.12.002
- 540 9. Christopher M, Bowd C, Belghith A, et al. Deep Learning Approaches Predict
541 Glaucomatous Visual Field Damage from OCT Optic Nerve Head En Face Images
542 and Retinal Nerve Fiber Layer Thickness Maps. *Ophthalmology.* 2020;127(3):346-
543 356. doi:10.1016/j.ophtha.2019.09.036
- 544 10. Hashimoto Y, Asaoka R, Kiwaki T, et al. Deep learning model to predict visual field
545 in central 10° from optical coherence tomography measurement in glaucoma. *Br J*
546 *Ophthalmol.* 2021;105(4):507-513. doi:10.1136/bjophthalmol-2019-315600
- 547 11. Hemelings R, Elen B, Barbosa-Breda J, et al. Pointwise Visual Field Estimation
548 From Optical Coherence Tomography in Glaucoma Using Deep Learning. *Transl Vis*
549 *Sci Technol.* 2022;11(8):22. doi:10.1167/tvst.11.8.22

- 550 12. Mariottoni EB, Datta S, Dov D, et al. Artificial Intelligence Mapping of Structure to
551 Function in Glaucoma. *Transl Vis Sci Technol.* 2020;9(2):19. doi:10.1167/tvst.9.2.19
- 552 13. Park K, Kim J, Lee J. A deep learning approach to predict visual field using optical
553 coherence tomography. *PloS One.* 2020;15(7):e0234902.
554 doi:10.1371/journal.pone.0234902
- 555 14. Tan O, Greenfield DS, Francis BA, Varma R, Schuman JS, Huang D. Estimating
556 Visual Field Mean Deviation using Optical Coherence Tomographic Nerve Fiber
557 Layer Measurements in Glaucoma Patients. *Sci Rep.* 2019;9(1):18528.
558 doi:10.1038/s41598-019-54792-w
- 559 15. Zhu H, Crabb DP, Schlottmann PG, et al. Predicting visual function from the
560 measurements of retinal nerve fiber layer structure. *Invest Ophthalmol Vis Sci.*
561 2010;51(11):5657-5666. doi:10.1167/iovs.10-5239
- 562 16. Yu HH, Maetschke SR, Antony BJ, et al. Estimating Global Visual Field Indices in
563 Glaucoma by Combining Macula and Optic Disc OCT Scans Using 3-Dimensional
564 Convolutional Neural Networks. *Ophthalmol Glaucoma.* 2021;4(1):102-112.
565 doi:10.1016/j.ogla.2020.07.002
- 566 17. Mwanza JC, Chang RT, Budenz DL, et al. Reproducibility of peripapillary retinal
567 nerve fiber layer thickness and optic nerve head parameters measured with cirrus
568 HD-OCT in glaucomatous eyes. *Invest Ophthalmol Vis Sci.* 2010;51(11):5724-5730.
569 doi:10.1167/iovs.10-5222
- 570 18. Carpineto P, Nubile M, Agnifili L, et al. Reproducibility and repeatability of Cirrus™
571 HD-OCT peripapillary retinal nerve fibre layer thickness measurements in young
572 normal subjects. *Ophthalmol J Int Ophthalmol Int J Ophthalmol Z Augenheilkd.*
573 2012;227(3):139-145. doi:10.1159/000334967
- 574 19. Gürses-Ozden R, Teng C, Vessani R, Zafar S, Liebmann JM, Ritch R. Macular and
575 retinal nerve fiber layer thickness measurement reproducibility using optical
576 coherence tomography (OCT-3). *J Glaucoma.* 2004;13(3):238-244.
577 doi:10.1097/00061198-200406000-00012
- 578 20. Garcia-Martin E, Pinilla I, Idoipe M, Fuertes I, Pueyo V. Intra and interoperator
579 reproducibility of retinal nerve fibre and macular thickness measurements using
580 Cirrus Fourier-domain OCT. *Acta Ophthalmol (Copenh).* 2011;89(1):e23-e29.
581 doi:10.1111/j.1755-3768.2010.02045.x
- 582 21. Tattersall CL, Vernon SA, Menon GJ. Mean deviation fluctuation in eyes with stable
583 Humphrey 24-2 visual fields. *Eye.* 2007;21(3):362-366. doi:10.1038/sj.eye.6702206
- 584 22. Wall M, Doyle CK, Zamba KD, Artes P, Johnson CA. The repeatability of mean
585 defect with size III and size V standard automated perimetry. *Invest Ophthalmol Vis*
586 *Sci.* 2013;54(2):1345-1351. doi:10.1167/iovs.12-10299

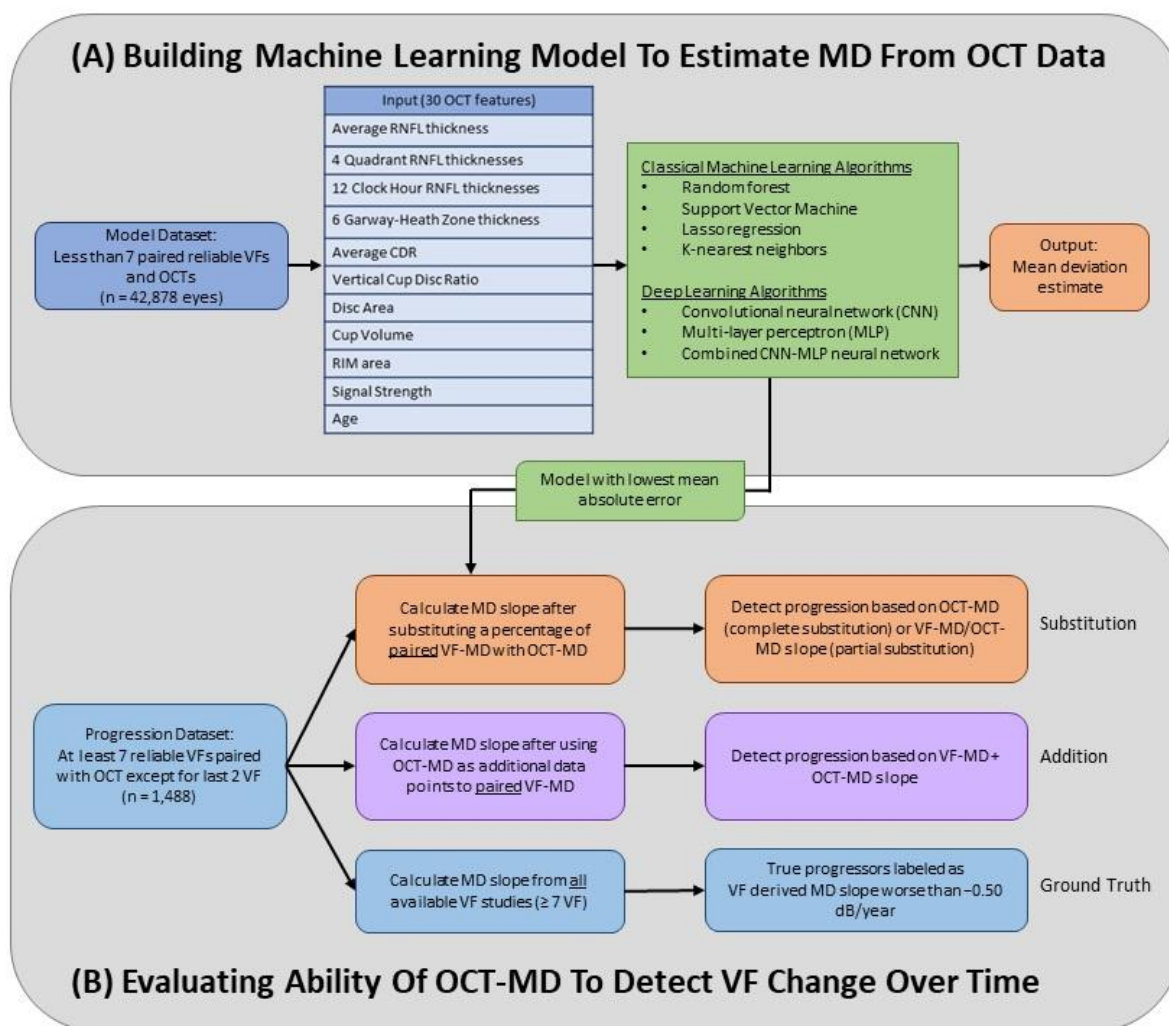
- 587 23. Krakau CET. A statistical trap in the evaluation of visual field decay. *Acta*
588 *Ophthalmol (Copenh)*. 1985;63(S173):19-21. doi:10.1111/j.1755-
589 3768.1985.tb06830.x
- 590 24. Nouri-Mahdavi K, Caprioli J, Coleman AL, Hoffman D, Gaasterland D. Pointwise
591 Linear Regression for Evaluation of Visual Field Outcomes and Comparison With
592 the Advanced Glaucoma Intervention Study Methods. *Arch Ophthalmol*.
593 2005;123(2):193-199. doi:10.1001/archophth.123.2.193
- 594 25. Mwanza JC, Kim HY, Budenz DL, et al. Residual and Dynamic Range of Retinal
595 Nerve Fiber Layer Thickness in Glaucoma: Comparison of Three OCT Platforms.
596 *Invest Ophthalmol Vis Sci*. 2015;56(11):6344-6351. doi:10.1167/iovs.15-17248
- 597 26. Structure-function Relationship in Advanced Glaucoma After R... : Journal of
598 Glaucoma. Accessed December 15, 2022.
599 [https://journals.lww.com/glaucomajournal/Fulltext/2019/11000/Structure_function_R](https://journals.lww.com/glaucomajournal/Fulltext/2019/11000/Structure_function_Relationship_in_Advanced.10.aspx)
600 [elationship_in_Advanced.10.aspx](https://journals.lww.com/glaucomajournal/Fulltext/2019/11000/Structure_function_Relationship_in_Advanced.10.aspx)
- 601 27. Mwanza JC, Kim HY, Budenz DL, et al. Residual and Dynamic Range of Retinal
602 Nerve Fiber Layer Thickness in Glaucoma: Comparison of Three OCT Platforms.
603 *Invest Ophthalmol Vis Sci*. 2015;56(11):6344-6351. doi:10.1167/iovs.15-17248
- 604 28. Seibold LK, Mandava N, Kahook MY. Comparison of Retinal Nerve Fiber Layer
605 Thickness in Normal Eyes Using Time-Domain and Spectral-Domain Optical
606 Coherence Tomography. *Am J Ophthalmol*. 2010;150(6):807-814.e1.
607 doi:10.1016/j.ajo.2010.06.024
- 608 29. Yohannan J, Wang J, Brown J, et al. Evidence-based Criteria for Assessment of
609 Visual Field Reliability. *Ophthalmology*. 2017;124(11):1612-1620.
610 doi:10.1016/j.ophtha.2017.04.035
- 611 30. De Moraes CGV, Juthani VJ, Liebmann JM, et al. Risk Factors for Visual Field
612 Progression in Treated Glaucoma. *Arch Ophthalmol*. 2011;129(5):562-568.
613 doi:10.1001/archophthalmol.2011.72
- 614 31. Chauhan BC, Garway-Heath DF, Goni FJ, et al. Practical recommendations for
615 measuring rates of visual field change in glaucoma. *Br J Ophthalmol*.
616 2008;92(4):569-573. doi:10.1136/bjo.2007.135012
- 617 32. Rabiolo A, Morales E, Mohamed L, et al. Comparison of Methods to Detect and
618 Measure Glaucomatous Visual Field Progression. *Transl Vis Sci Technol*.
619 2019;8(5):2. doi:10.1167/tvst.8.5.2
- 620 33. Hou K, Bradley C, Herbert P, et al. Predicting Visual Field Worsening with
621 Longitudinal Optical Coherence Tomography Data Using a Gated Transformer
622 Network. *Ophthalmology*. Published online March 30, 2023.
623 doi:10.1016/j.ophtha.2023.03.019

- 624 34. Guo Z, Kwon YH, Lee K, et al. Optical Coherence Tomography Analysis Based
625 Prediction of Humphrey 24-2 Visual Field Thresholds in Patients With Glaucoma.
626 *Invest Ophthalmol Vis Sci.* 2017;58(10):3975-3985. doi:10.1167/iovs.17-21832
- 627 35. Wong D, Chua J, Bujor I, et al. Comparison of machine learning approaches for
628 structure–function modeling in glaucoma. *Ann N Y Acad Sci.* 2022;1515(1):237-248.
629 doi:10.1111/nyas.14844
- 630 36. Yu HH, Maetschke SR, Antony BJ, et al. Estimating Global Visual Field Indices in
631 Glaucoma by Combining Macula and Optic Disc OCT Scans Using 3-Dimensional
632 Convolutional Neural Networks. *Ophthalmol Glaucoma.* 2021;4(1):102-112.
633 doi:10.1016/j.ogla.2020.07.002
- 634 37. Lazaridis G, Montesano G, Afgeh SS, et al. Predicting Visual Fields From Optical
635 Coherence Tomography via an Ensemble of Deep Representation Learners. *Am J*
636 *Ophthalmol.* 2022;238:52-65. doi:10.1016/j.ajo.2021.12.020
- 637 38. Bogunović H, Kwon YH, Rashid A, et al. Relationships of Retinal Structure and
638 Humphrey 24-2 Visual Field Thresholds in Patients With Glaucoma. *Invest*
639 *Ophthalmol Vis Sci.* 2015;56(1):259-271. doi:10.1167/iovs.14-15885
- 640 39. Rabiolo A, Morales E, Afifi AA, Yu F, Nouri-Mahdavi K, Caprioli J. Quantification of
641 Visual Field Variability in Glaucoma: Implications for Visual Field Prediction and
642 Modeling. *Transl Vis Sci Technol.* 2019;8(5):25. doi:10.1167/tvst.8.5.25
- 643 40. Taketani Y, Murata H, Fujino Y, Mayama C, Asaoka R. How Many Visual Fields Are
644 Required to Precisely Predict Future Test Results in Glaucoma Patients When
645 Using Different Trend Analyses? *Invest Ophthalmol Vis Sci.* 2015;56(6):4076-4082.
646 doi:10.1167/iovs.14-16341
- 647 41. Sehi M, Goharian I, Konduru R, et al. Retinal blood flow in glaucomatous eyes with
648 single-hemifield damage. *Ophthalmology.* 2014;121(3):750-758.
649 doi:10.1016/j.ophtha.2013.10.022
- 650 42. Yoshioka T, Song Y, Kawai M, et al. Retinal blood flow reduction in normal-tension
651 glaucoma with single-hemifield damage by Doppler optical coherence tomography.
652 *Br J Ophthalmol.* 2021;105(1):124-130. doi:10.1136/bjophthalmol-2019-315616
- 653 43. Kamalipour A, Moghimi S, Khosravi P, et al. Combining Optical Coherence
654 Tomography and Optical Coherence Tomography Angiography Longitudinal Data
655 for the Detection of Visual Field Progression in Glaucoma. *Am J Ophthalmol.*
656 2023;246:141-154. doi:10.1016/j.ajo.2022.10.016
- 657 44. Wong D, Chua J, Tan B, et al. Combining OCT and OCTA for Focal Structure–
658 Function Modeling in Early Primary Open-Angle Glaucoma. *Invest Ophthalmol Vis*
659 *Sci.* 2021;62(15):8. doi:10.1167/iovs.62.15.8

- 660 45. Belghith A, Medeiros FA, Bowd C, et al. Structural Change Can Be Detected in
661 Advanced-Glaucoma Eyes. *Invest Ophthalmol Vis Sci.* 2016;57(9):OCT511-518.
662 doi:10.1167/iovs.15-18929
- 663 46. Bowd C, Zangwill LM, Weinreb RN, Medeiros FA, Belghith A. Estimating OCT
664 Structural Measurement Floors to Improve Detection of Progression In Advanced
665 Glaucoma. *Am J Ophthalmol.* 2017;175:37-44. doi:10.1016/j.ajo.2016.11.010
- 666 47. Lavinsky F, Wu M, Schuman JS, et al. Can Macula and Optic Nerve Head
667 Parameters Detect Glaucoma Progression in Eyes with Advanced Circumpapillary
668 Retinal Nerve Fiber Layer Damage? *Ophthalmology.* 2018;125(12):1907-1912.
669 doi:10.1016/j.ophtha.2018.05.020
- 670 48. Drance SM. The early field defects in glaucoma. *Invest Ophthalmol.* 1969;8(1):84-
671 91.
- 672 49. Nicholas SP, Werner EB. Location of early glaucomatous visual field defects. *Can J*
673 *Ophthalmol J Can Ophthalmol.* 1980;15(3):131-133.
- 674 50. Ancil JL, Anderson DR. Early foveal involvement and generalized depression of the
675 visual field in glaucoma. *Arch Ophthalmol Chic Ill 1960.* 1984;102(3):363-370.
676 doi:10.1001/archopht.1984.01040030281019
- 677 51. Heijl A, Lundqvist L. The frequency distribution of earliest glaucomatous visual field
678 defects documented by automatic perimetry. *Acta Ophthalmol (Copenh).*
679 1984;62(4):658-664. doi:10.1111/j.1755-3768.1984.tb03979.x
- 680 52. Schiefer U, Papageorgiou E, Sample PA, et al. Spatial pattern of glaucomatous
681 visual field loss obtained with regionally condensed stimulus arrangements. *Invest*
682 *Ophthalmol Vis Sci.* 2010;51(11):5685-5689. doi:10.1167/iovs.09-5067
- 683 53. Hood DC, Raza AS, de Moraes CGV, Liebmann JM, Ritch R. Glaucomatous
684 damage of the macula. *Prog Retin Eye Res.* 2013;32C:1-21.
685 doi:10.1016/j.preteyeres.2012.08.003
- 686 54. Arvanitaki V, Tsilimbaris MK, Pallikaris A, et al. Macular Retinal and Nerve Fiber
687 Layer Thickness in Early Glaucoma: Clinical Correlations. *Middle East Afr J*
688 *Ophthalmol.* 2012;19(2):204-210. doi:10.4103/0974-9233.95251
- 689 55. Xu L, Asaoka R, Kiwaki T, et al. Predicting the Glaucomatous Central 10-Degree
690 Visual Field From Optical Coherence Tomography Using Deep Learning and Tensor
691 Regression. *Am J Ophthalmol.* 2020;218:304-313. doi:10.1016/j.ajo.2020.04.037
- 692 56. Nouri-Mahdavi K, Mohammadzadeh V, Rabiolo A, Edalati K, Caprioli J, Yousefi S.
693 Prediction of Visual Field Progression from OCT Structural Measures in Moderate to
694 Advanced Glaucoma. *Am J Ophthalmol.* 2021;226:172-181.
695 doi:10.1016/j.ajo.2021.01.023

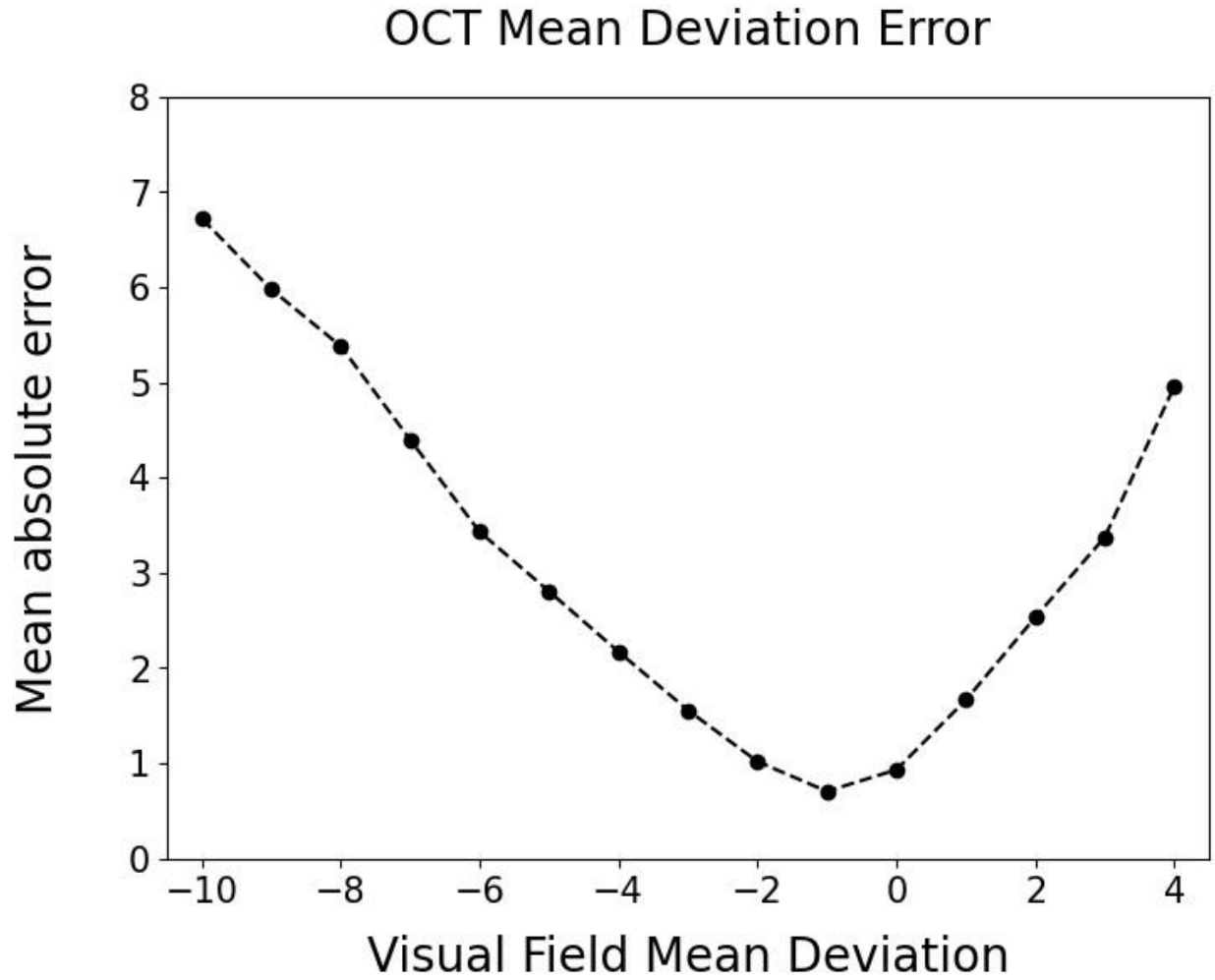
- 696 57. Medeiros FA, Zangwill LM, Alencar LM, et al. Detection of glaucoma progression
697 with stratus OCT retinal nerve fiber layer, optic nerve head, and macular thickness
698 measurements. *Invest Ophthalmol Vis Sci.* 2009;50(12):5741-5748.
699 doi:10.1167/iovs.09-3715
- 700 58. Herbert P, Hou K, Bradley C, et al. Forecasting Risk of Future Rapid Glaucoma
701 Worsening Using Early Visual Field, Optical Coherence Tomography, and Clinical
702 Data. *Ophthalmol Glaucoma.* Published online March 19, 2023:S2589-
703 4196(23)00063-7. doi:10.1016/j.ogla.2023.03.005
- 704 59. Pham AT, Ramulu PY, Boland MV, Yohannan J. The Effect of Transitioning from
705 SITA Standard to SITA Faster on Visual Field Performance. *Ophthalmology.*
706 2021;128(10):1417-1425. doi:10.1016/j.ophtha.2021.03.032
- 707 60. Le CT, Fiksel J, Ramulu P, Yohannan J. Differences in visual field loss pattern when
708 transitioning from SITA standard to SITA faster. *Sci Rep.* 2022;12(1):7001.
709 doi:10.1038/s41598-022-11044-8
- 710 61. Heijl A, Patella VM, Chong LX, et al. A New SITA Perimetric Threshold Testing
711 Algorithm: Construction and a Multicenter Clinical Study. *Am J Ophthalmol.*
712 2019;198:154-165. doi:10.1016/j.ajo.2018.10.010
- 713 62. Mendieta N, Suárez J, Blasco C, Muñoz R, Pueyo C. A Comparative Study between
714 Swedish Interactive Thresholding Algorithm Faster and Swedish Interactive
715 Thresholding Algorithm Standard in Glaucoma Patients. *J Curr Ophthalmol.*
716 2021;33(3):247-252. doi:10.4103/joco.joco_148_20
- 717 63. Phu J, Kalloniatis M. A Strategy for Seeding Point Error Assessment for Retesting
718 (SPEAR) in Perimetry Applied to Normal Subjects, Glaucoma Suspects, and
719 Patients With Glaucoma. *Am J Ophthalmol.* 2021;221:115-130.
720 doi:10.1016/j.ajo.2020.07.047
- 721 64. Chauhan BC, Malik R, Shuba LM, Rafuse PE, Nicolela MT, Artes PH. Rates of
722 Glaucomatous Visual Field Change in a Large Clinical Population. *Invest*
723 *Ophthalmol Vis Sci.* 2014;55(7):4135-4143. doi:10.1167/iovs.14-14643
- 724

725 **Tables and Figures:**



726

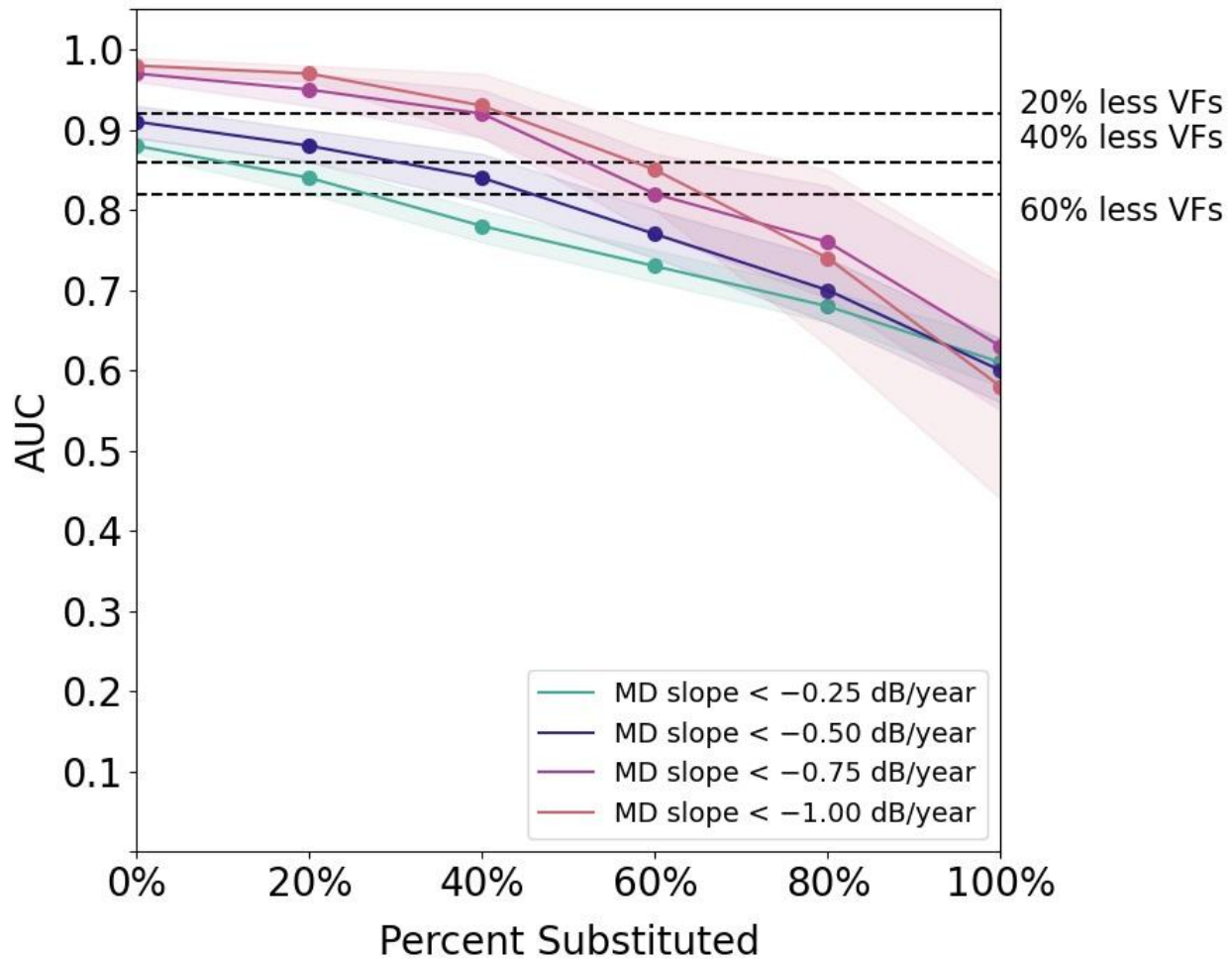
727 Figure 1: (A) Various models were built using data obtained from OCT scans to
 728 estimate a corresponding MD. (B) We then compared the ability to detect glaucoma
 729 progression using OCT-MD estimates with VF-MD measurements to using only VF-MD
 730 alone. To establish a ground truth for both, eyes were labeled true progressors if the
 731 MD slope calculated from all available VF studies (equating to at least 2 or more
 732 additional data points) was worse than -0.50 dB/year.



733

734 Figure 2: Mean absolute error of OCT-MD estimates across a range of VF-MD
735 measurements

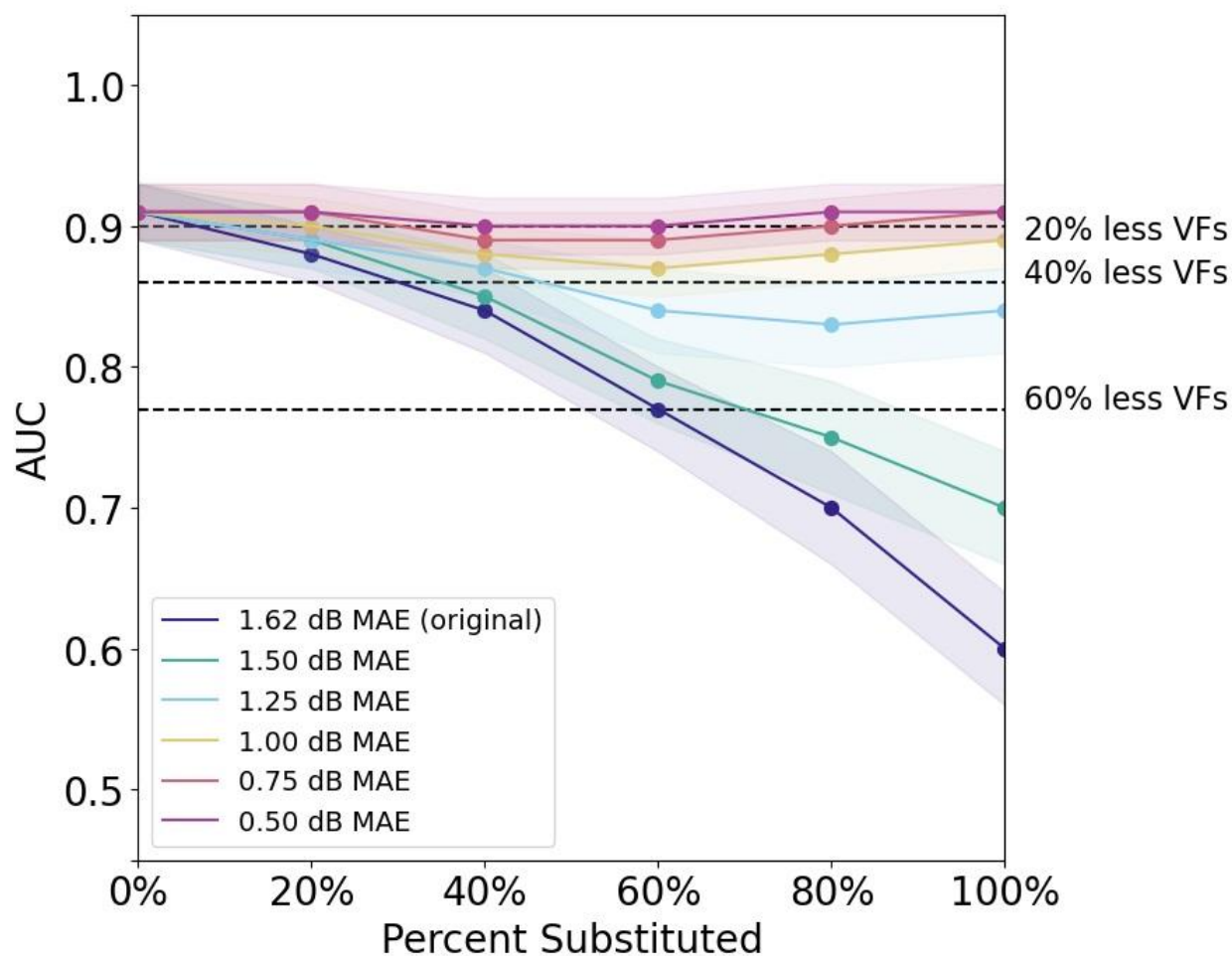
VF-MD/OCT-MD Performance



736

737 Figure 3: The predictive ability of VF-MD/OCT-MD slope calculated with different
738 percentages substitution for various MD-slope cutoff thresholds. Substitution of 0%
739 represents the performance of MD slopes calculated only from VF-MD (baseline VF-MD
740 slope). A substitution of 100% represents the performance of MD slopes calculated from
741 only OCT-MD. Dashed lines represent the performance of baseline VF-MD slopes using
742 20%, 40%, and 60% fewer VFs.

Error Simulation for VF-MD/OCT-MD



743

744 Figure 4: The predictive ability of VF-MD/OCT-MD slope with various levels of accuracy
745 ranging from MAE of 0.50 to 1.50 dB. A substitution of 0% represents the performance
746 of MD slopes calculated only from VF-MD (baseline VF-MD slope). A substitution of
747 100% represents the performance of MD slopes calculated from only OCT-MD. Dashed
748 lines represent the performance of baseline VF-MD slopes using 20%, 40%, and 60%
749 fewer VFs.

750 Table 1: Baseline demographic, VF, OCT characteristics

	Model dataset (n = 44,659)	Progression dataset (n=4,044)
Mean age (SD), years	62 (15)	64 (11)
Gender		
Male, n	18,860 (42%)	1,715 (42%)
Female, n	25,794 (58%)	2,329 (58%)
Race		
White or Caucasian, n	24,413 (58%)	2,305 (57%)
Black or African American, n	13,068 (29%)	1,360 (34%)
Asian, n	3,220 (7.2%)	196 (4.9%)
American Indian or Alaska Native, n	150 (0.34%)	9 (0.22%)
Pacific Islander, n	48 (0.11%)	4 (0.10%)
Hispanic, n	2 (0.00%)	0 (0%)
Other, n	2,643 (5.9%)	125 (3.1%)
Unknown, n	1,115 (2.5%)	45 (1.1%)
Glaucoma Severity		
Suspect, n	15,000 (34%)	2,065 (51%)
Mild, n	25,984 (58%)	1,796 (44%)
Moderate, n	3,675 (8.2%)	183 (4.5%)
VF Characteristics		
Mean MD (SD), dB	-1.86 (2.54)	-1.59 (2.22)
Mean PSD (SD), dB	2.56 (1.89)	2.46 (1.72)
OCT Characteristics		
Mean RNFL (SD), μm	86 (12)	83 (11)
Mean CDR (SD)	0.60 (0.16)	0.62 (0.15)

751 * SD = standard deviation, MD = mean deviation, PSD = pattern standard deviation,
 752 RNFL = retinal nerve fiber thickness layer, CDR = cup-to-disc-ratio, VF = visual field,
 753 OCT = optical coherence tomography

754

755 Table 2: OCT-MD Support Vector Machine regression performance metrics

	Mean absolute error (dB)	% within 0.25 dB	% within 0.5 dB	% within 1 dB	% within 2 dB	% within 4 dB
Overall (n = 12,222)	1.62	11%	21%	41%	71%	93%
Suspect (n = 5,973)	1.36	12%	24%	44%	77%	98%
Mild (n = 5,337)	1.48	11%	21%	43%	72%	95%
Moderate (n = 912)	5.55	1.5 %	2.4%	3.9%	8.2%	21%

756 * OCT-MD = OCT derived mean deviation estimates; n = the number of OCT-VF pairs
757 from each dataset